Electronic Supporting Information (ESI)

Unique Chemistry of Thiuram Polysulfides Enable Energy Dense Lithium Batteries

Amruth Bhargav,[a] Ying Ma*[d], Kollur Shashikala,[a] Yi Cui,[ac] Yaroslav Losovyj,[e] and Yongzhu Fu*[ab]

[a]*Department of Mechanical Engineering, Indiana University-Purdue University Indianapolis, Indianapolis, IN 46202, USA*

[b]*School of Chemistry and Molecular Engineering, Zhengzhou University, Zhengzhou, Henan 450001, P.R. China, E-mail: yfu@zzu.edu.cn*

[c]*School of Mechanical Engineering, Purdue University, West Lafayette, IN 47907, USA*

[d]*Materials Science and Engineering, University of Wisconsin-Eau Claire, Eau Claire, WI 54702, USA. E-mail: yingma@uwec.edu*

[e]*Department of Chemistry, Indiana University, Bloomington, IN 47405, USA*

Supplementary data:

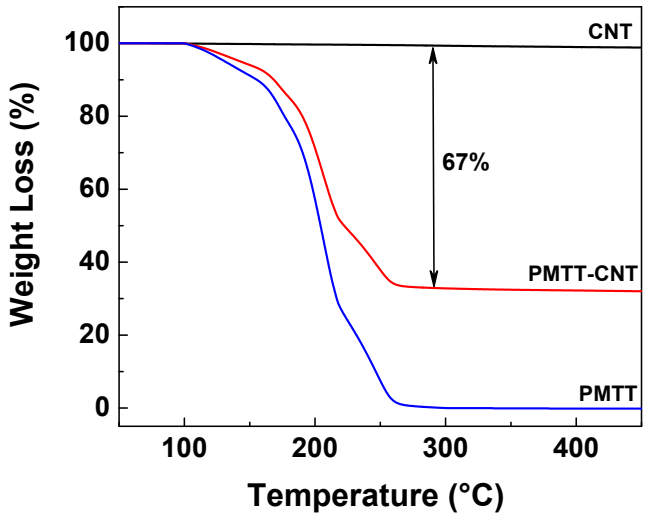

Figure S1. Thermogravimetric analysis (TGA) of a representative batch of PMTT-CNT cathode along with that of pure CNT and PMTT as the baseline showing that 67% of the cathode consists of PMTT.

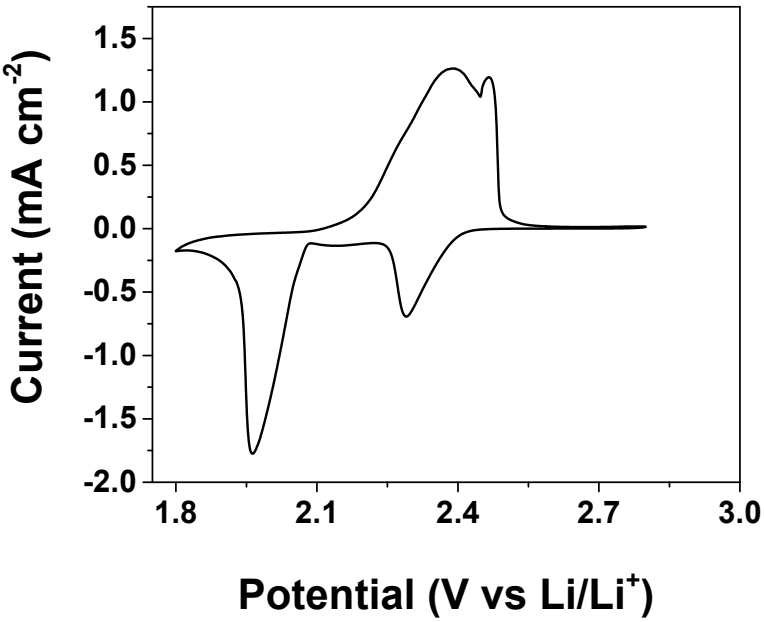

Figure S2. Cyclic voltammogram of sulfur cathode. The potential was swept from open circuit voltage (OCV) to 1.8 V and then swept back to 2.8 V at a scanning rate of 0.05 mV s^{-1}.

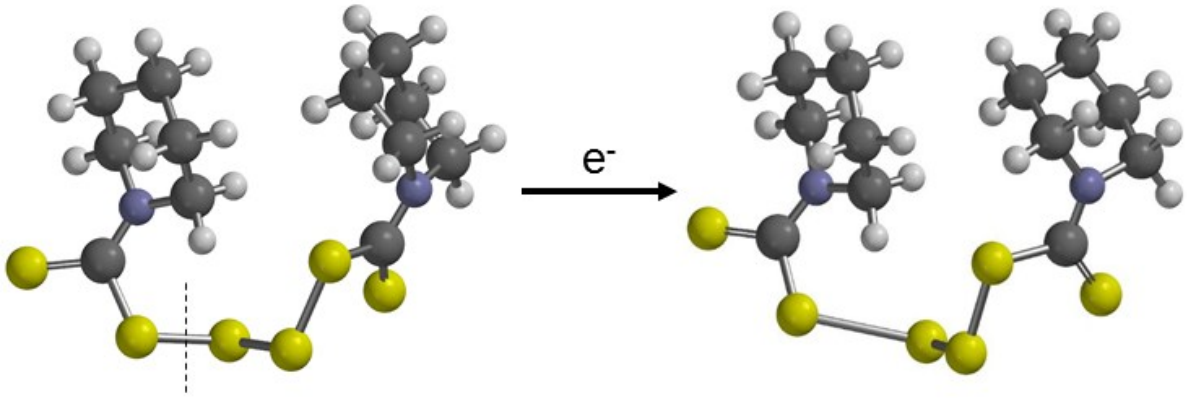

Figure S3. Addition of an electron to PMTT (left) at the S-S bond indicated yields the unstable structure (right).

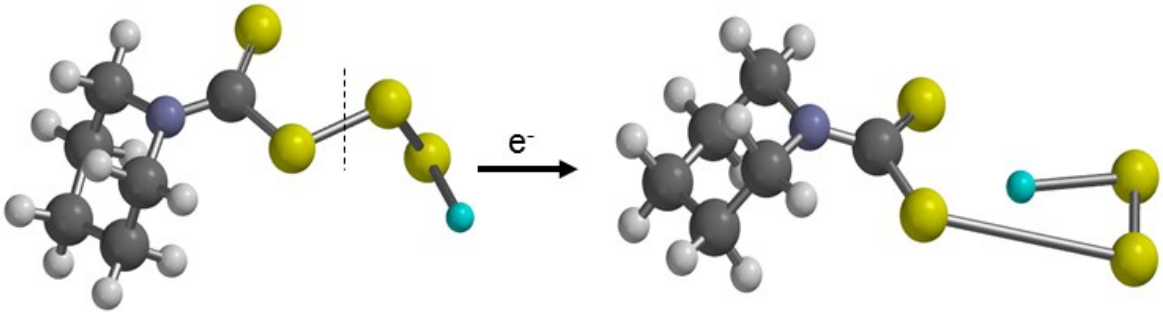

Figure S4. Addition of an electron to intermediate **4** (left) at the S-S bond indicated yields the unstable structure (right).

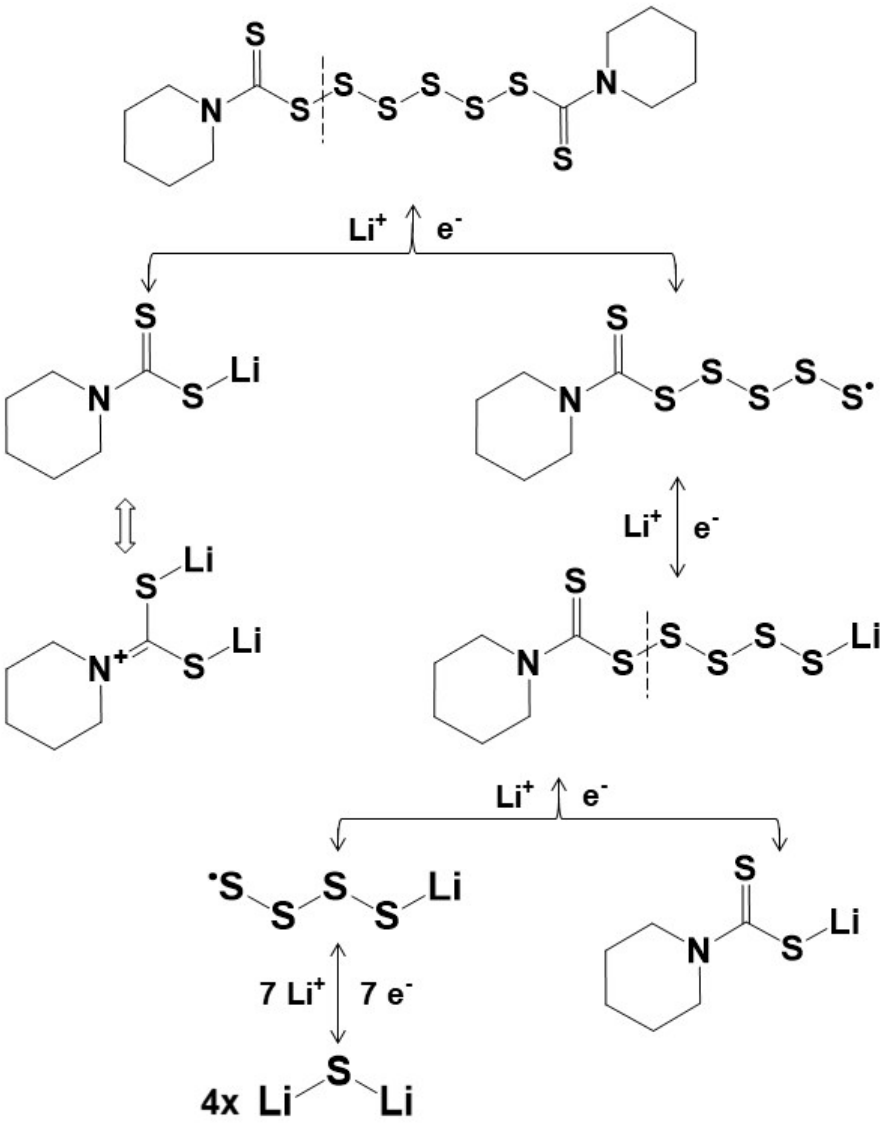

Figure S5. Redox reactions of PMTH during battery cycling.

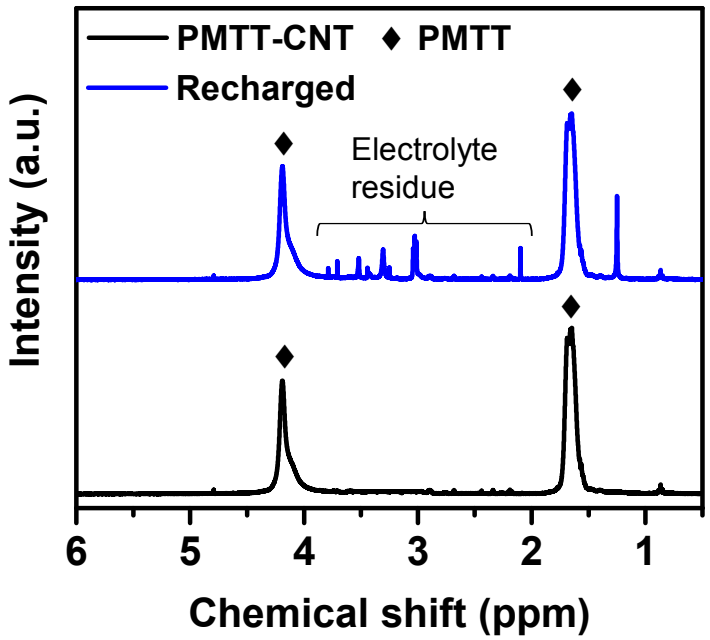

Figure S6. NMR spectrum of fresh PMTT-CNT cathode and after recharge. PMTT peaks were referenced from the Spectral Database for Organic Compounds (SDBS) by the National Institute of Advanced Industrial Science and Technology. (Source: http://sdbs.db.aist.go.jp/sdbs/cgi-bin/direct_frame_disp.cgi?sdbsno=7145)

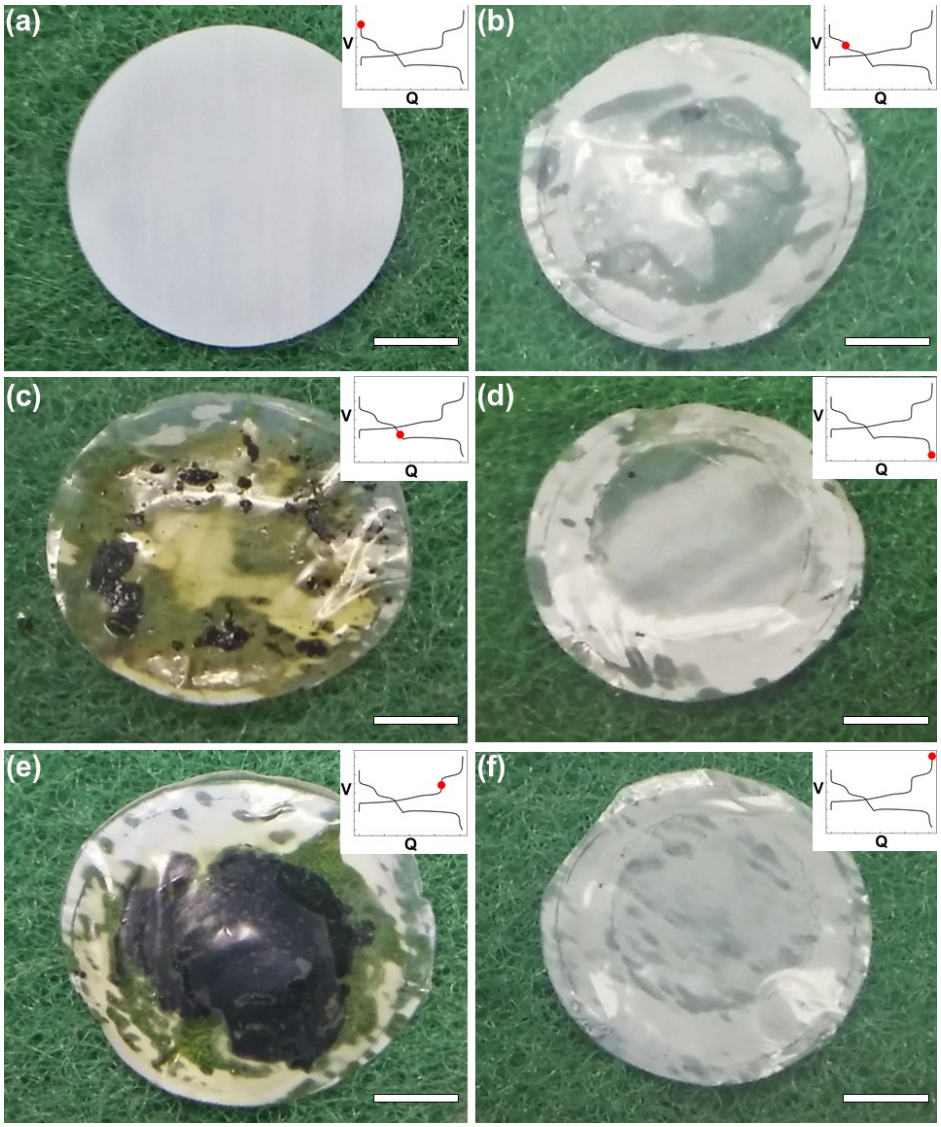

Figure S7. Optical images of the separators taken from the cell at different stages of cycling as represented by the insert figure. All scale bars roughly represent 5 mm.

Figure S8. Optical images of the lithium metal anode extracted from the cell containing PMTH cathode after 100 cycles. Mossy and uneven Li deposition including dendrite formation leading to premature cell failure can be visibly observed.

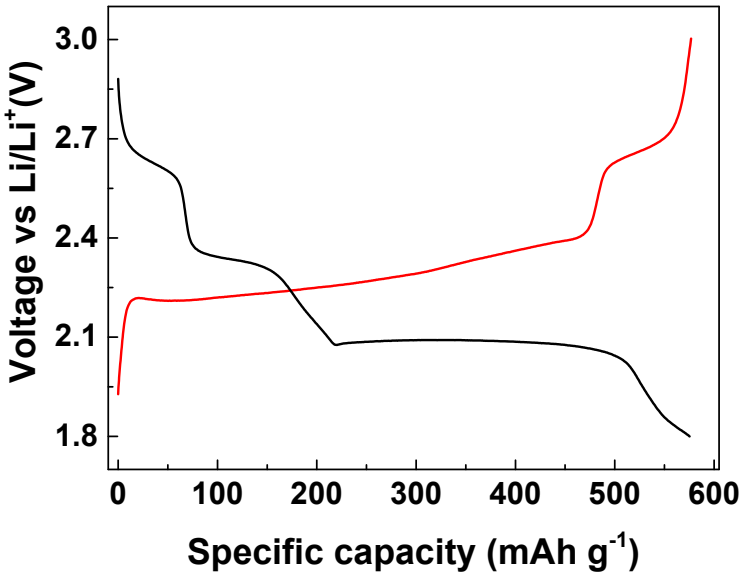

Figure S9. Voltage profile of PMTH-CNT cathode cycled at C/5. The active material (PMTH) loading on the cathode was 6 mg cm^{-2}. The cycling rate was based on PMTH mass in the cathode with 1C = 597 mA g^{-1}.

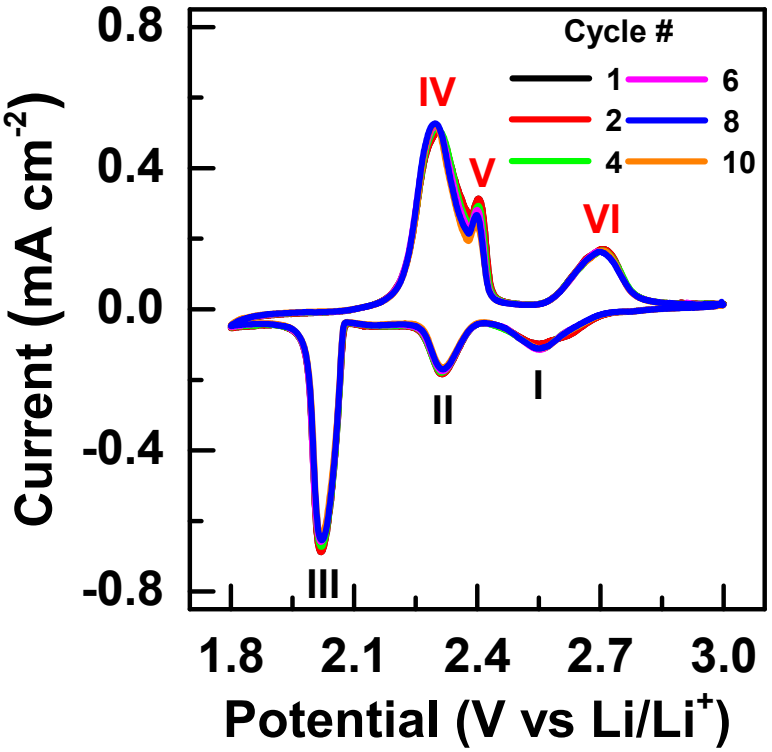

Figure S10. Cyclic voltammogram of PMTH-CNT cathode. The potential was swept from open circuit voltage (OCV) to 1.8 V and then swept back to 3.0 V at a scanning rate of 0.05 mV s^{-1}.

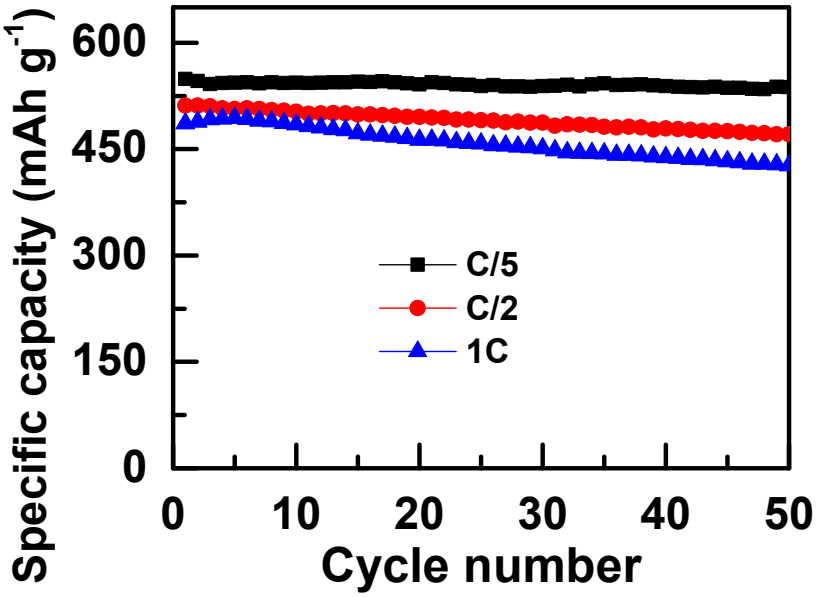

Figure S11. Rate performance of PMTH-CNT cathode. The cycling rate was based on PMTH mass in the cathode with 1C = 597 mA g^{-1}.

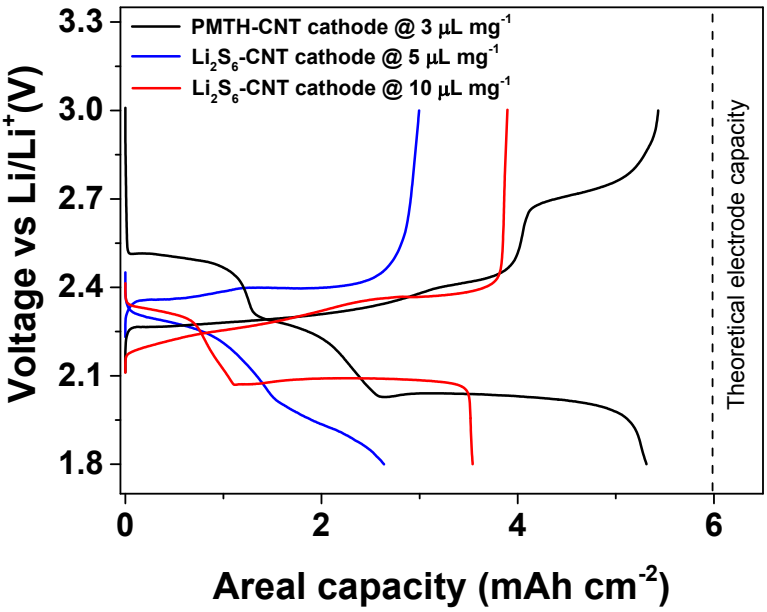

Figure S12. Comparison of performance of high loading PMTH cathode (PMTH loading of 10 mg cm^{-2}) with sulfur cathodes at different electrolyte to sulfur ratios. The cells were cycled at the same current density.